

000
 001
 002
 003
 004 **Supplementary Material to “External Prior Guided Internal Prior Learning for**
 005 **Real Noisy Image Denoising”**
 006
 007
 008
 009
 010
 011
 012
 013
 014
 015
 016
 017
 018
 019
 020
 021
 022
 023
 024
 025
 026
 027
 028
 029
 030
 031
 032
 033
 034
 035
 036
 037
 038
 039
 040
 041
 042
 043
 044
 045
 046
 047
 048
 049
 050
 051
 052
 053

054
 055
 056
 057
 058
 059
 060
 061
 062
 063
 064
 065
 066
 067
 068
 069
 070
 071
 072
 073
 074
 075
 076
 077
 078
 079
 080
 081
 082
 083
 084
 085
 086
 087
 088
 089
 090
 091
 092
 093
 094
 095
 096
 097
 098
 099
 100
 101
 102
 103
 104
 105
 106
 107

Anonymous CVPR submission

Paper ID 1047

In this supplementary material, we provide:

1. The closed-form solution of the proposed weighted sparse coding model in the main paper.
2. More denoising results on the real noisy images (with no “ground truth”) provided in the dataset [1].
3. More denoising results on the 15 cropped real noisy images (with “ground truth”) used in the dataset [2].
4. More denoising results on the 60 cropped real noisy images (with “ground truth”) from [2].

1. Closed-Form Solution of the Weighted Sparse Coding Problem (4)

The weighted sparse coding problem in the main paper is:

$$\min_{\alpha} \|\mathbf{y} - \mathbf{D}\alpha\|_2^2 + \|\mathbf{w}^T \alpha\|_1. \quad (1)$$

Since \mathbf{D} is an orthonormal matrix, problem (1) is equivalent to

$$\min_{\alpha} \|\mathbf{D}^T \mathbf{y} - \alpha\|_2^2 + \|\mathbf{w}^T \alpha\|_1. \quad (2)$$

For simplicity, we denote $\mathbf{z} = \mathbf{D}^T \mathbf{y}$. Since $\mathbf{w}_i = c * 2\sqrt{2}\sigma^2 / (\Lambda_i + \varepsilon)$ is positive (please refer to Eq. (18) in the main paper), problem (2) can be written as

$$\min_{\alpha} \sum_{i=1}^{p^2} ((\mathbf{z}_i - \alpha_i)^2 + \mathbf{w}_i |\alpha_i|). \quad (3)$$

The problem (3) is separable w.r.t. α_i and can be simplified to p^2 scalar minimization problems

$$\min_{\alpha_i} (\mathbf{z}_i - \alpha_i)^2 + \mathbf{w}_i |\alpha_i|, \quad (4)$$

where $i = 1, \dots, p^2$. Taking derivative of α_i in problem (4) and setting the derivative to be zero. There are two cases for the solution.

(a) If $\alpha_i \geq 0$, we have

$$2(\alpha_i - \mathbf{z}_i) + \mathbf{w}_i = 0. \quad (5)$$

The solution is

$$\hat{\alpha}_i = \mathbf{z}_i - \frac{\mathbf{w}_i}{2} \geq 0. \quad (6)$$

So $\mathbf{z}_i \geq \frac{\mathbf{w}_i}{2} > 0$, and the solution $\hat{\alpha}_i$ can be written as

$$\hat{\alpha}_i = \text{sgn}(\mathbf{z}_i) * (|\mathbf{z}_i| - \frac{\mathbf{w}_i}{2}), \quad (7)$$

where $\text{sgn}(\bullet)$ is the sign function.

(b) If $\alpha_i < 0$, we have

$$2(\alpha_i - \mathbf{z}_i) - \mathbf{w}_i = 0. \quad (8)$$

The solution is

$$\hat{\alpha}_i = \mathbf{z}_i + \frac{\mathbf{w}_i}{2} < 0. \quad (9)$$

So $\mathbf{z}_i < -\frac{\mathbf{w}_i}{2} < 0$, and the solution $\hat{\alpha}_i$ can be written as

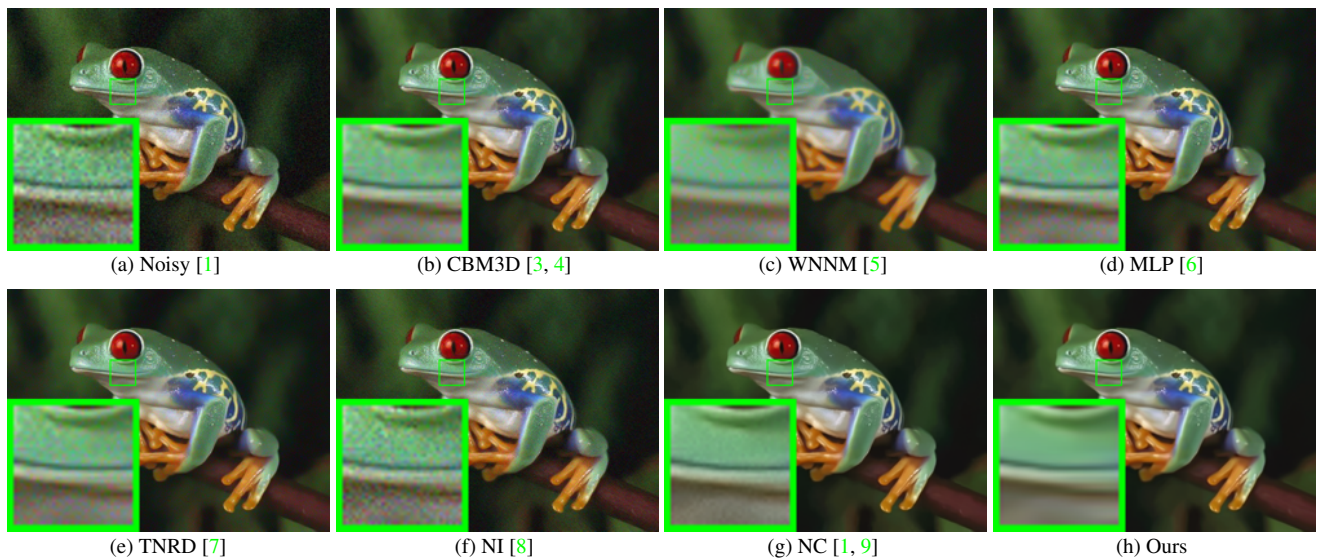
$$\hat{\alpha}_i = \text{sgn}(\mathbf{z}_i) * (-\mathbf{z}_i - \frac{\mathbf{w}_i}{2}) = \text{sgn}(\mathbf{z}_i) * (|\mathbf{z}_i| - \frac{\mathbf{w}_i}{2}). \quad (10)$$

108 In summary, we have the final solution of the weighted sparse coding problem (1) as
 109
 110 $\hat{\alpha} = \text{sgn}(\mathbf{D}^T \mathbf{y}) \odot \max(|\mathbf{D}^T \mathbf{y}| - \mathbf{w}/2, 0),$ (11)

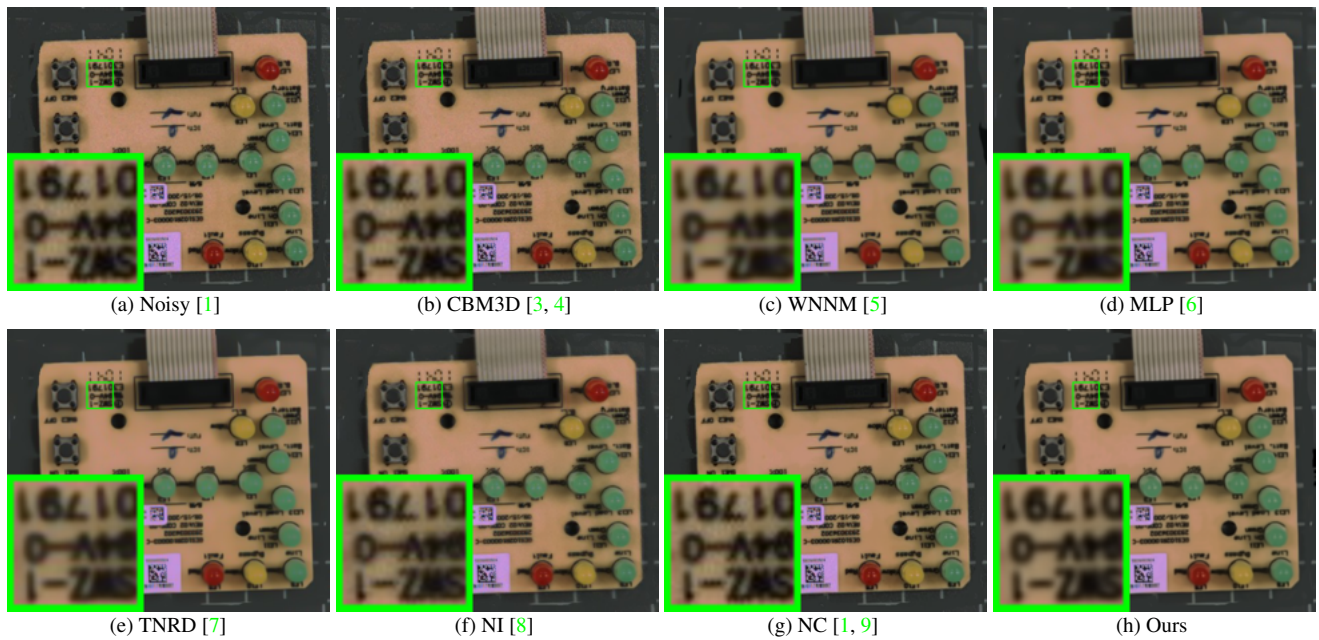
111 where \odot means element-wise multiplication and $|\mathbf{D}^T \mathbf{y}|$ is the absolute value of each entry of the vector $\mathbf{D}^T \mathbf{y}.$

112 2. More Results on Real Noisy Images in [1]

114 In this section, we give more visual comparisons of the competing methods on the real noisy images provided in [1]. The
 115 real noisy images in this dataset [1] have no “ground truth” images and hence we only compare the visual quality of the
 116 denoised images by different methods. As can be seen from Figures 1-4, our proposed method performs better than the state-
 117 of-the-art denoising methods. This validates the effectiveness of our proposed external prior guided internal prior learning
 118 framework for real noisy image denoising.
 119



138 Figure 1. Denoised images of the real noisy image “Frog” [1] by different methods. The images are better to be zoomed in on screen.
 139



161 Figure 2. Denoised images of the real noisy image “Circuit” [1] by different methods. The images are better to be zoomed in on screen.
 162

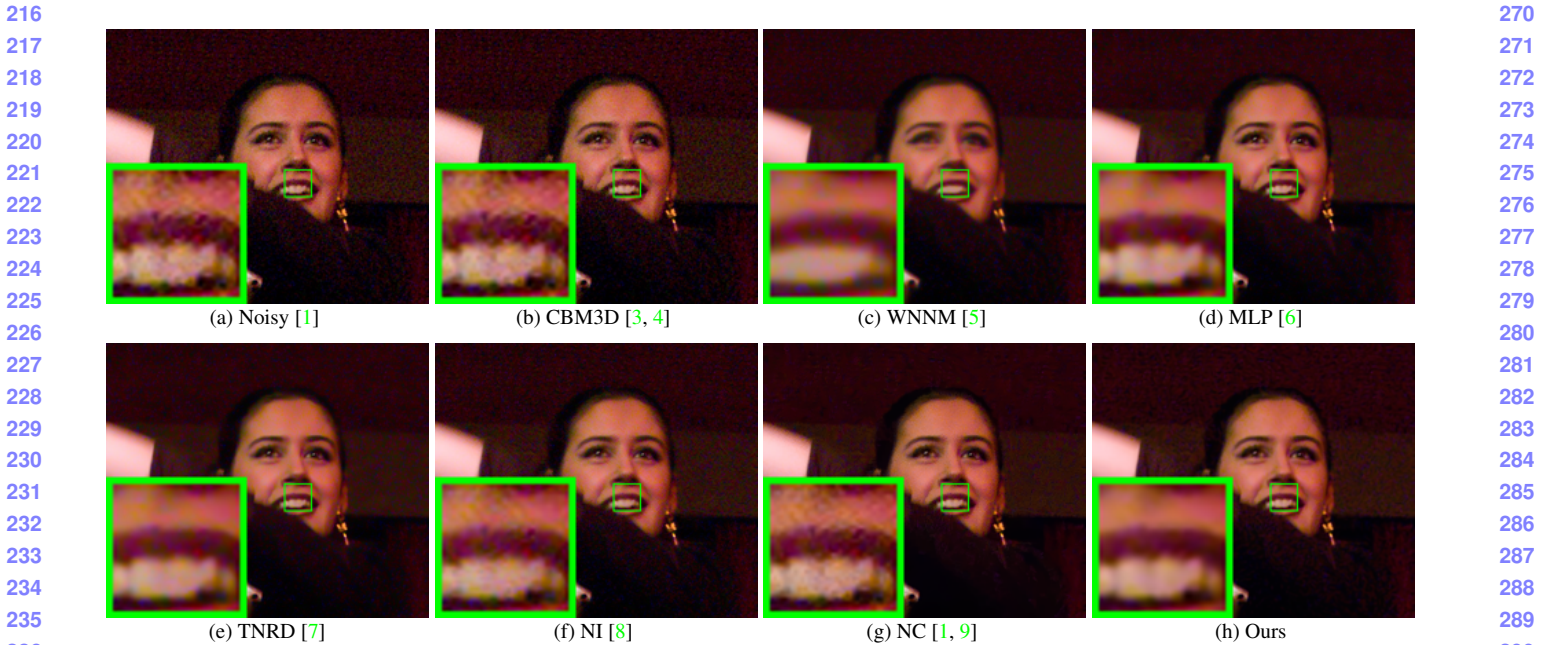


Figure 3. Denoised images of the real noisy image “Woman” [1] by different methods. The images are better to be zoomed in on screen.

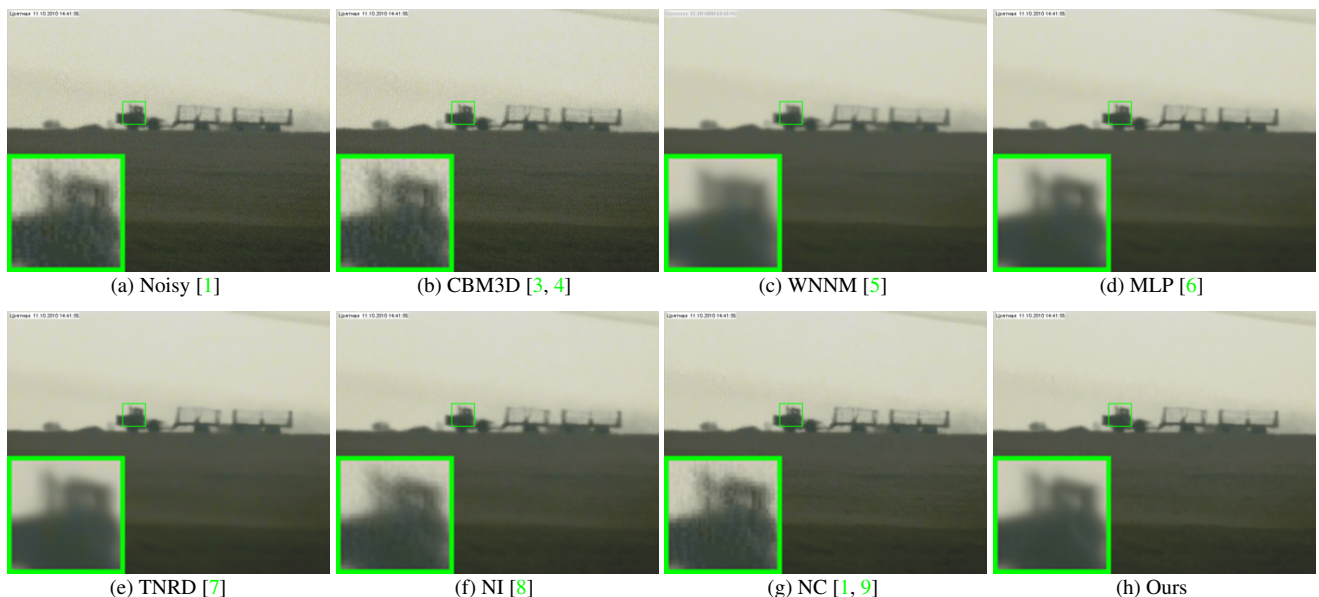


Figure 4. Denoised images of the real noisy image “Vehicle” [1] by different methods. The images are better to be zoomed in on screen.

3. More Results on the 15 Cropped Images Used in [2]

In this section, we provide more visual comparisons of the proposed method with the state-of-the-art denoising methods on the 15 cropped real noisy images used in [2]. As can be seen from Figures 5-9, on most cases, our proposed method achieves better performance than the competing methods. This validates the effectiveness of our proposed external prior guided internal prior learning framework for real noisy image denoising.

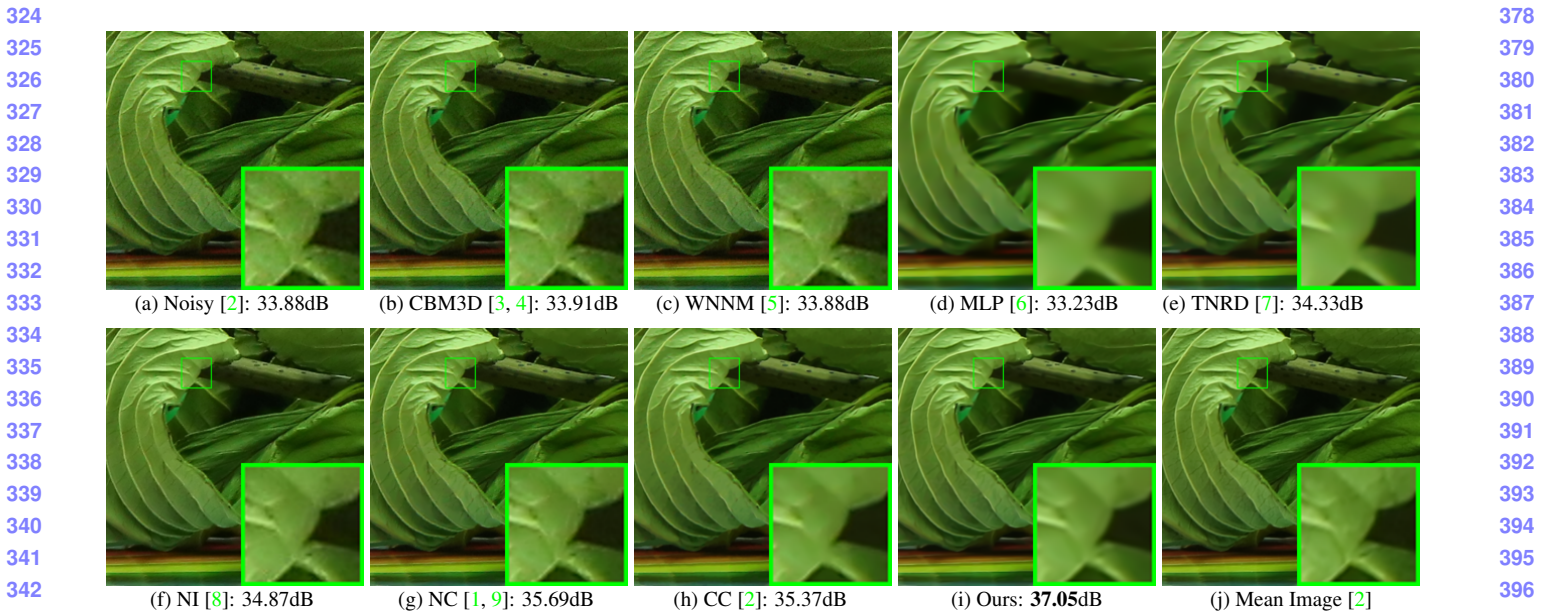


Figure 5. Denoised images of a region cropped from the real noisy image “Canon 5D Mark 3 ISO 3200 2” [2] by different methods. The images are better to be zoomed in on screen.

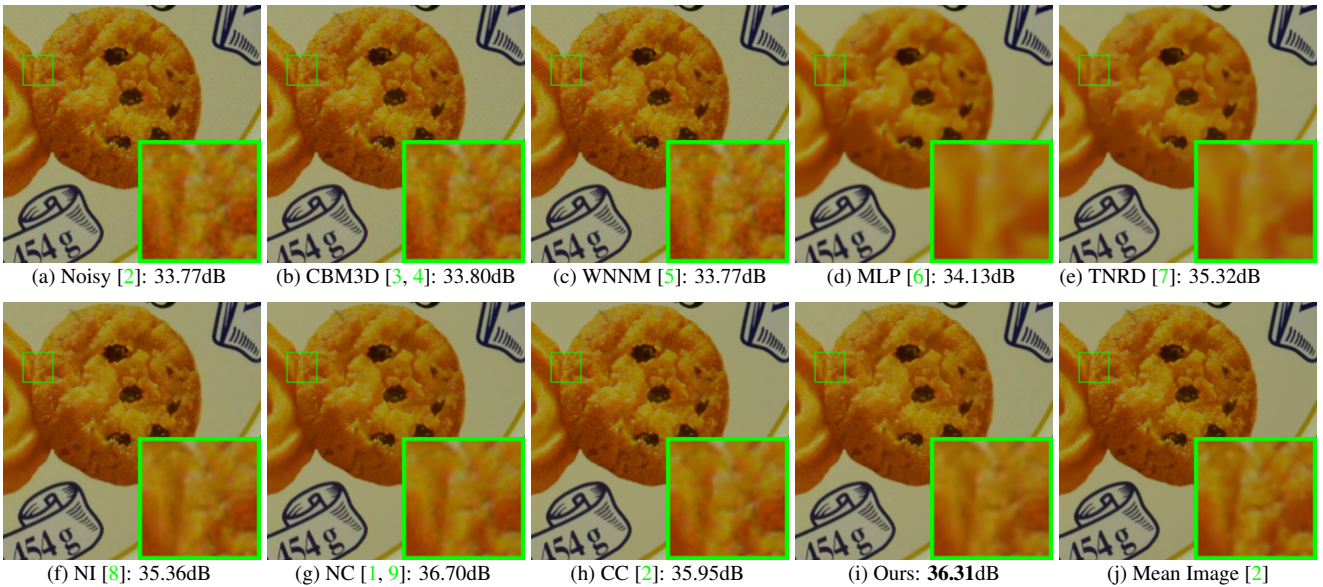


Figure 6. Denoised images of a region cropped from the real noisy image “Canon 5D Mark 3 ISO 3200 2” [2] by different methods. The images are better to be zoomed in on screen.

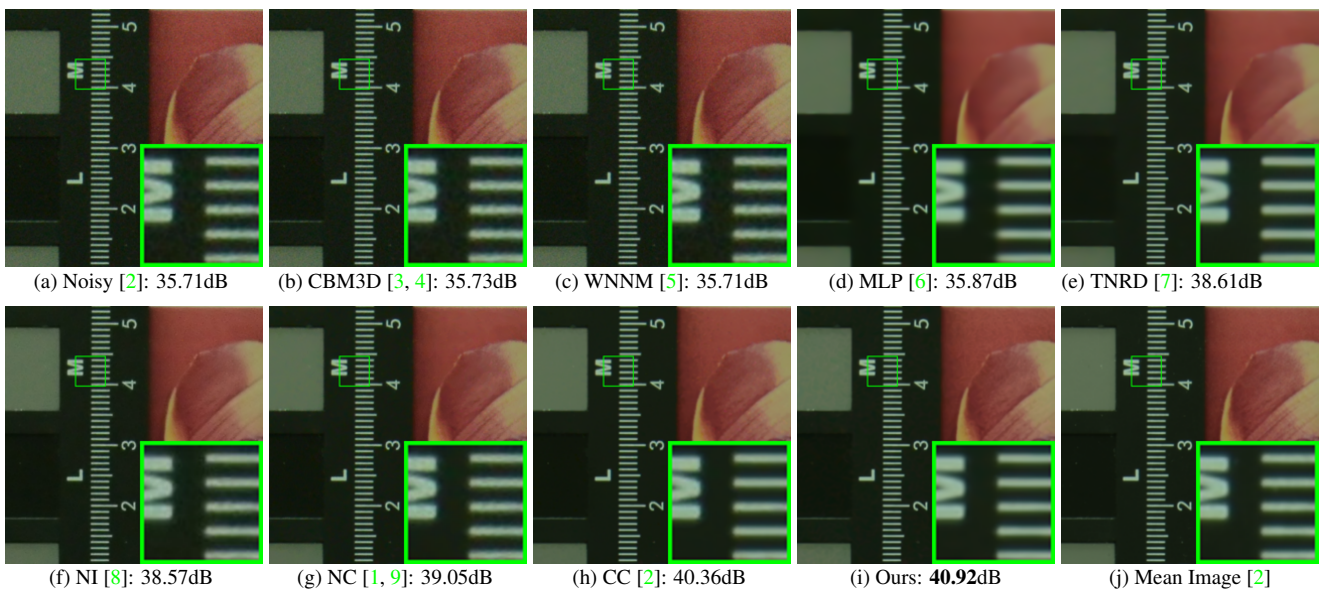


Figure 7. Denoised images of a region cropped from the real noisy image “Nikon D800 ISO 1600 2” [2] by different methods. The images are better to be zoomed in on screen.

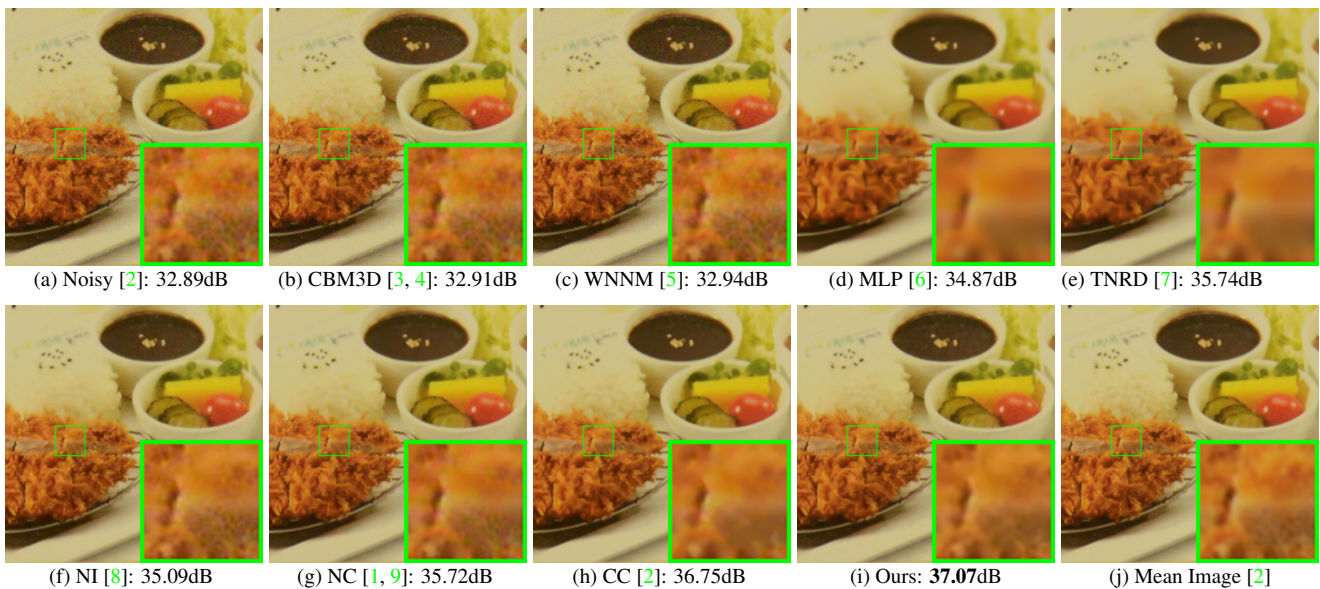


Figure 8. Denoised images of a region cropped from the real noisy image “Nikon D800 ISO 3200 2” [2] by different methods. The images are better to be zoomed in on screen.

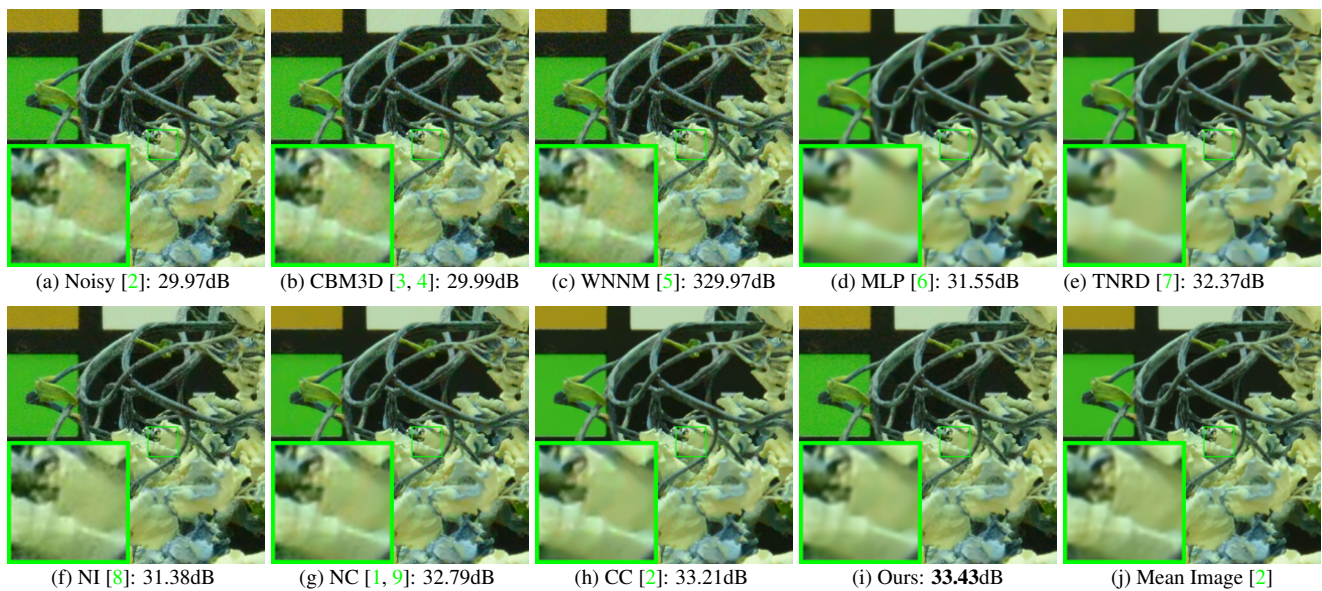


Figure 9. Denoised images of a region cropped from the real noisy image “Nikon D800 ISO 6400 2” [2] by different methods. The images are better to be zoomed in on screen.

4. More Results on the 60 Cropped Images in [2]

In this section, we provide more visual comparisons of the proposed method with the state-of-the-art denoising methods on the 60 cropped real noisy images we cropped from [2]. As can be seen from Figures 10-15, on most cases, our proposed method achieves better performance than the competing methods. This validates the effectiveness of our proposed external prior guided internal prior learning framework for real noisy image denoising.

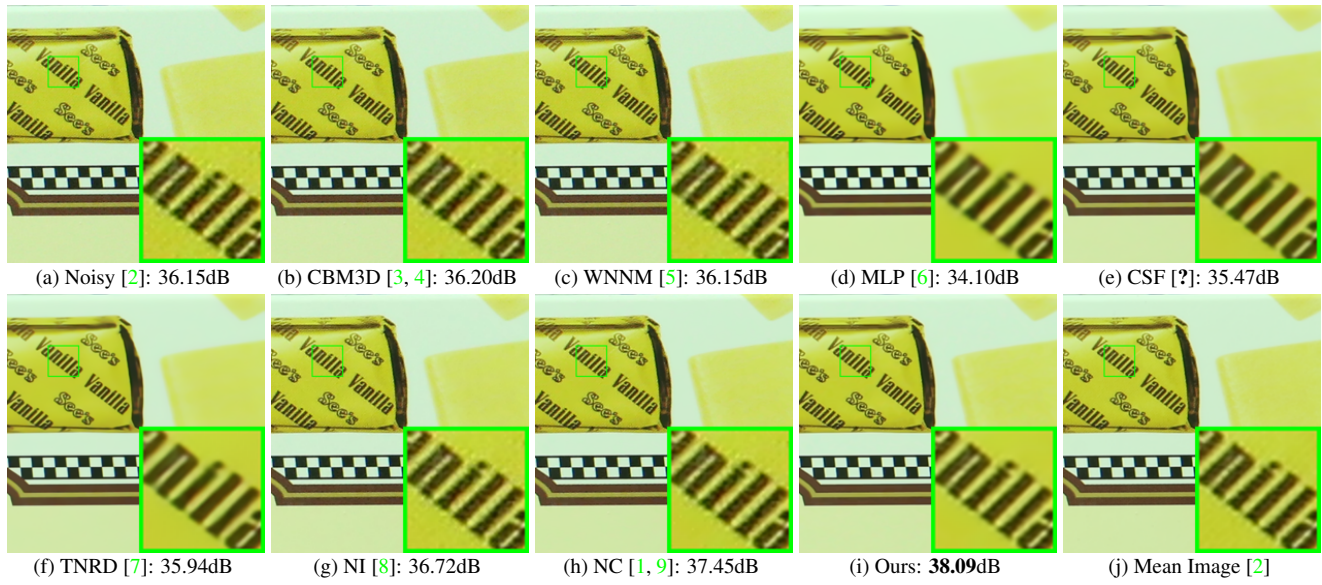


Figure 10. Denoised images of a region cropped from the real noisy image “Canon EOS 5D Mark3 ISO 3200 C1” [2] by different methods. The images are better viewed by zooming in on screen.

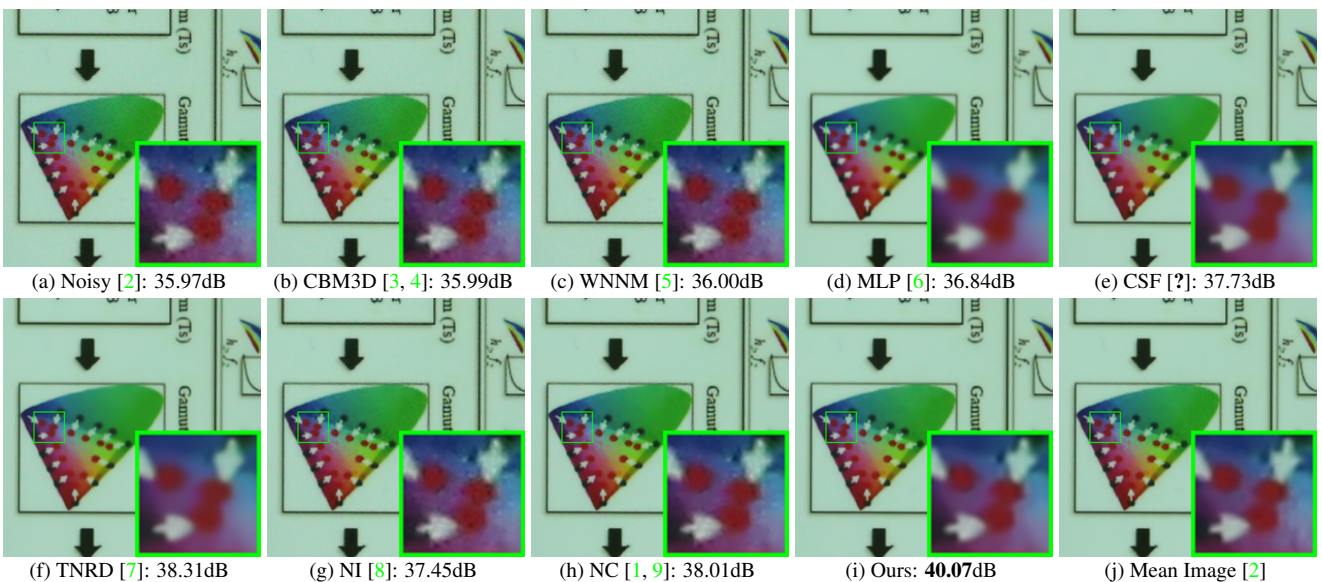


Figure 11. Denoised imagesupp of a region cropped from the real noisy image “Canon EOS 5D Mark3 ISO 3200 C2” [2] by different methods. The images are better viewed by zooming in on screen.

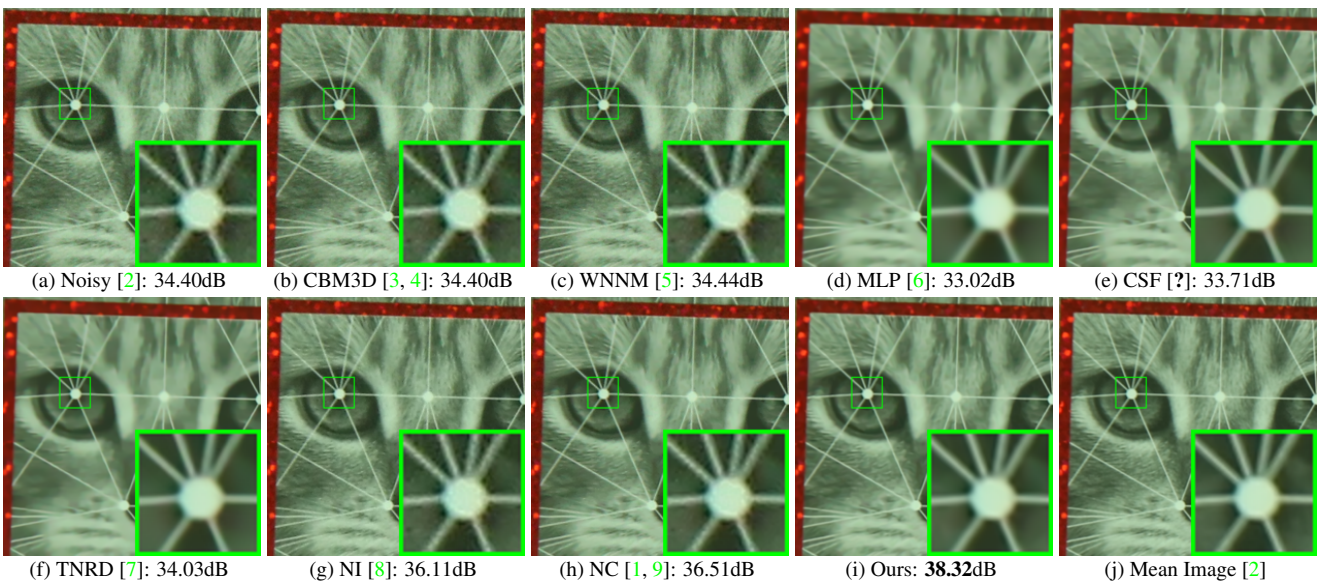


Figure 12. Denoised imagesupp of a region cropped from the real noisy image “Canon EOS 5D Mark3 ISO 3200 C3” [2] by different methods. The images are better viewed by zooming in on screen.

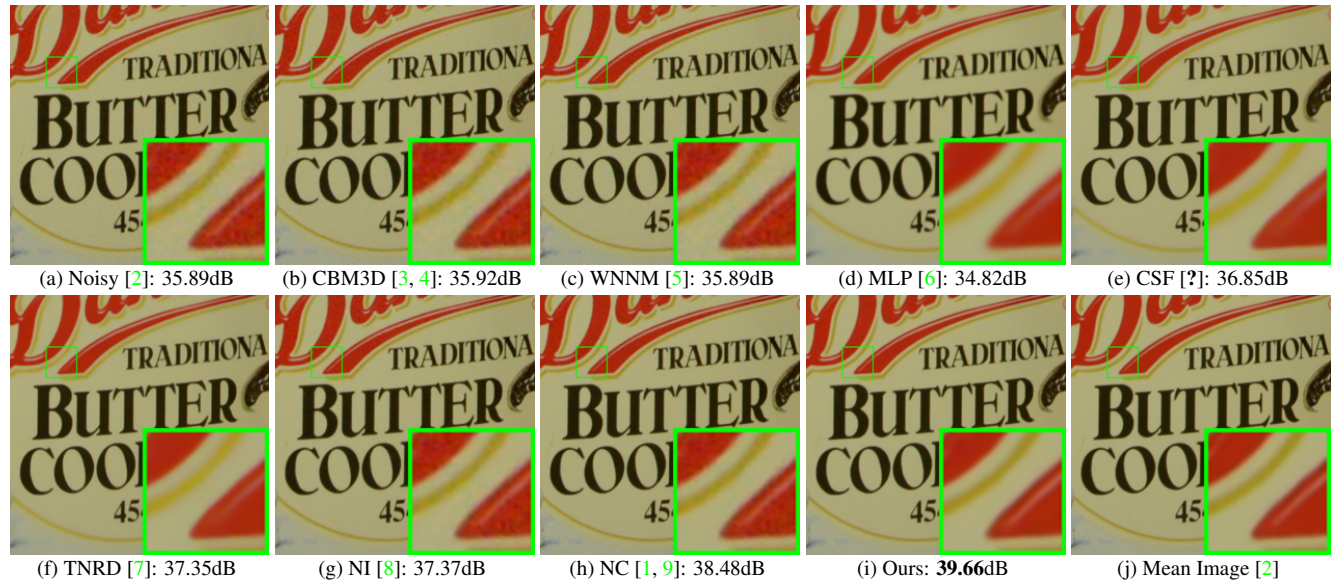


Figure 13. Denoised images of a region cropped from the real noisy image “Nikon D600 ISO 3200 C1” [2] by different methods. The images are better viewed by zooming in on screen.

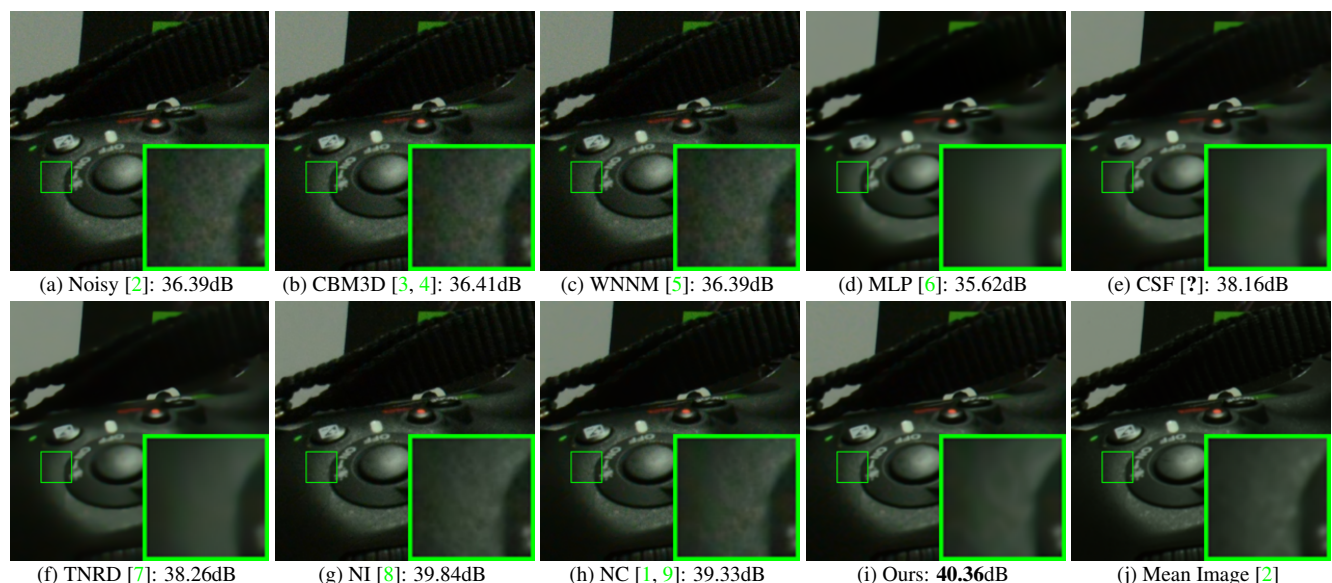


Figure 14. Denoised images of a region cropped from the real noisy image “Nikon D600 ISO 3200 C2” [2] by different methods. The images are better viewed by zooming in on screen.

810
811
812
813
814
815
816
817
818
819
820
821
822
823
824
825
826
827
828
829
830
831
832
833
834
835
836
837
838
839
840
841
842
843
844
845
846
847
848
849
850
851
852
853
854
855
856
857
858
859
860
861
862
863

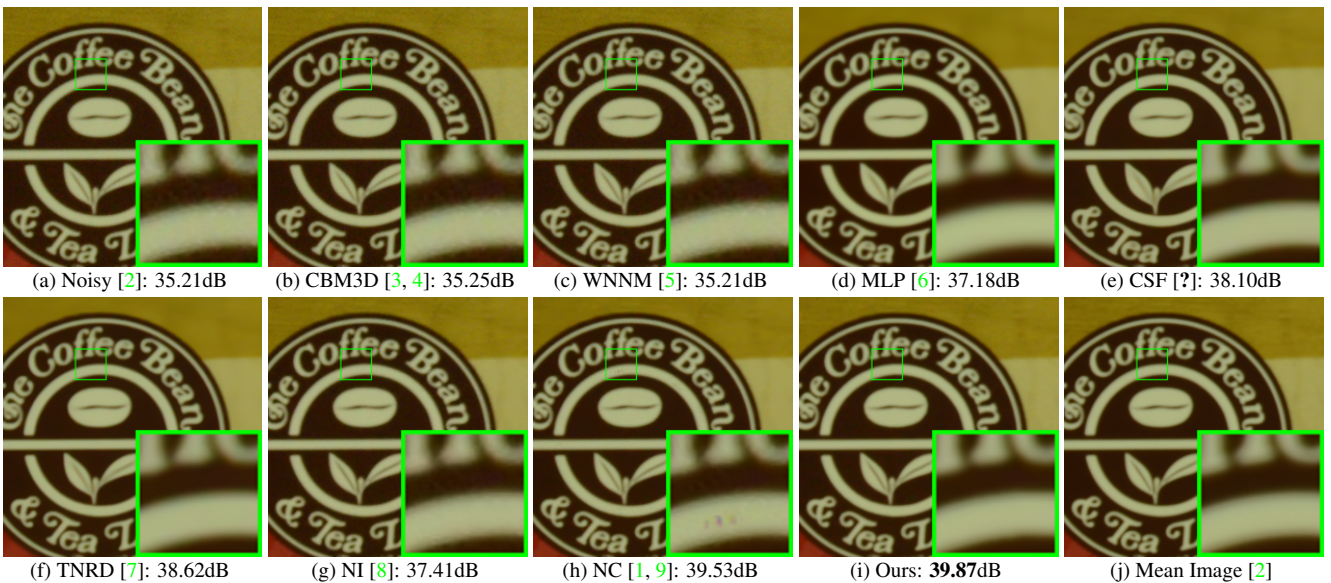


Figure 15. Denoised images of a region cropped from the real noisy image “Nikon D800 ISO 1600 B2” [2] by different methods. The images are better viewed by zooming in on screen.

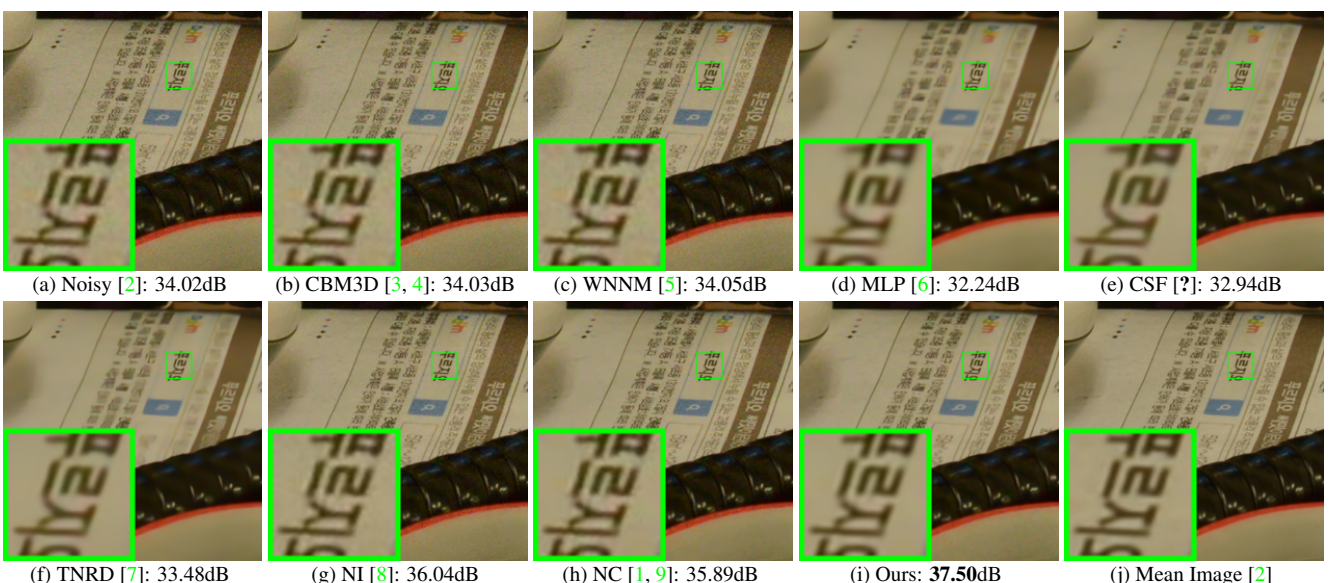


Figure 16. Denoised images of a region cropped from the real noisy image “Nikon D800 ISO 3200 A1” [2] by different methods. The images are better viewed by zooming in on screen.

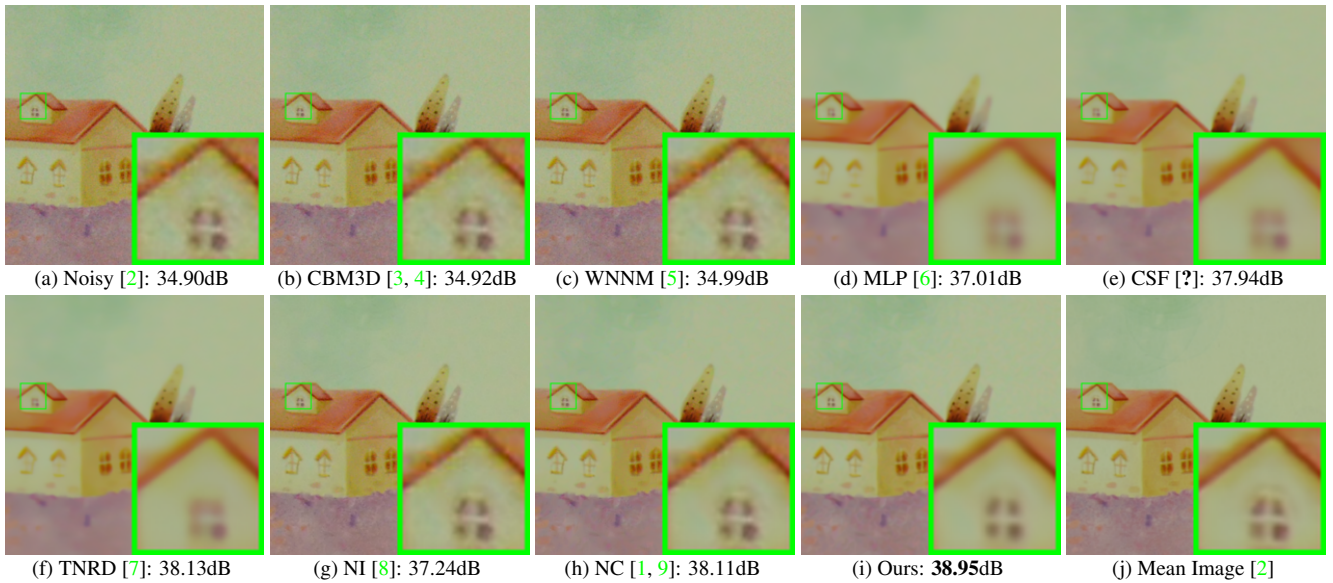


Figure 17. Denoised images of a region cropped from the real noisy image “Nikon D800 ISO 3200 A2” [2] by different methods. The images are better viewed by zooming in on screen.

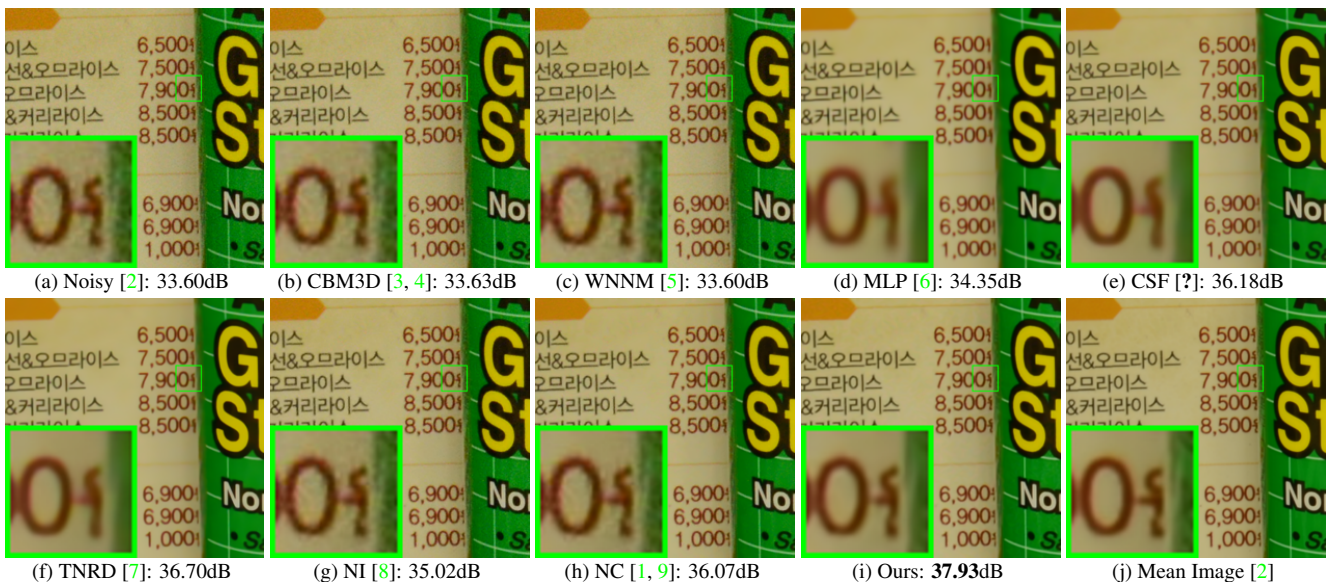


Figure 18. Denoised images of a region cropped from the real noisy image “Nikon D800 ISO 3200 A3” [2] by different methods. The images are better viewed by zooming in on screen.

References

- [1] M. Lebrun, M. Colom, and J. M. Morel. The noise clinic: a blind image denoising algorithm. <http://www.ipol.im/pub/art/2015/125/>. Accessed 01 28, 2015. 1, 2, 3, 4, 5, 6, 7, 8, 9, 10
- [2] S. Nam, Y. Hwang, Y. Matsushita, and S. J. Kim. A holistic approach to cross-channel image noise modeling and its application to image denoising. *IEEE Conference on Computer Vision and Pattern Recognition (CVPR)*, pages 1683–1691, 2016. 1, 3, 4, 5, 6, 7, 8, 9, 10
- [3] K. Dabov, A. Foi, V. Katkovnik, and K. Egiazarian. Image denoising by sparse 3-D transform-domain collaborative filtering. *IEEE Transactions on Image Processing*, 16(8):2080–2095, 2007. 2, 3, 4, 5, 6, 7, 8, 9, 10

- 1080 [4] K. Dabov, A. Foi, V. Katkovnik, and K. Egiazarian. Color image denoising via sparse 3D collaborative filtering with grouping 1134
1081 constraint in luminance-chrominance space. *IEEE International Conference on Image Processing (ICIP)*, pages 313–316, 2007. 2, 3, 1135
1082 4, 5, 6, 7, 8, 9, 10 1136
1083 [5] S. Gu, L. Zhang, W. Zuo, and X. Feng. Weighted nuclear norm minimization with application to image denoising. *IEEE Conference 1137
1084 on Computer Vision and Pattern Recognition (CVPR)*, pages 2862–2869, 2014. 2, 3, 4, 5, 6, 7, 8, 9, 10 1138
1085 [6] H. C. Burger, C. J. Schuler, and S. Harmeling. Image denoising: Can plain neural networks compete with BM3D? *IEEE Conference 1139
1086 on Computer Vision and Pattern Recognition (CVPR)*, pages 2392–2399, 2012. 2, 3, 4, 5, 6, 7, 8, 9, 10 1140
1087 [7] Y. Chen, W. Yu, and T. Pock. On learning optimized reaction diffusion processes for effective image restoration. *IEEE Conference on 1141
1088 Computer Vision and Pattern Recognition (CVPR)*, pages 5261–5269, 2015. 2, 3, 4, 5, 6, 7, 8, 9, 10 1142
1089 [8] Neatlab ABSsoft. Neat Image. <https://ni.neatvideo.com/home>. 2, 3, 4, 5, 6, 7, 8, 9, 10 1143
1090 [9] M. Lebrun, M. Colom, and J.-M. Morel. Multiscale image blind denoising. *IEEE Transactions on Image Processing*, 24(10):3149– 1145
1091 3161, 2015. 2, 3, 4, 5, 6, 7, 8, 9, 10 1146
1092
1093
1094
1095
1096
1097
1098
1099
1100
1101
1102
1103
1104
1105
1106
1107
1108
1109
1110
1111
1112
1113
1114
1115
1116
1117
1118
1119
1120
1121
1122
1123
1124
1125
1126
1127
1128
1129
1130
1131
1132
1133